Cellular and Molecular Biology
E-ISSN : 1165-158X / P-ISSN : 0145-5680
www.cellmolbiol.org

*Original Research*

# Electroacupuncture ameliorates spatial learning and memory impairment via attenuating NOX2-related oxidative stress in a rat model of Alzheimer's disease induced by $A\beta_{1-42}$

G. Wu[1], L. Li[1,2*], H-M. Li[1], Y. Zeng[1], W-C. Wu[2]

[1] Institute of Biomedical Engineering, School of Preclinical and Forensic Medicine, Sichuan University, Chengdu, 610041 Sichuan, P. R. China
[2] Laboratory of Cardiovascular Diseases, Regenerative Medicine Research Center, West China Hospital, Sichuan University, Chengdu, 610041 Sichuan, P. R. China

**Correspondence to:** lilianghx@163.com

**Received** October 18, 2016; **Accepted** March 1, 2017; **Published** April 29, 2017

**Doi:** http://dx.doi.org/10.14715/cmb/2017.63.4.7



**Abstract:** Alzheimer's disease (AD) is a chronic neurodegenerative disorder characterized by progressive deterioration of cognition and memory, in which oxidative stress has been played a crucial role in the pathology of AD. Electroacupuncture (EA) is a widely used therapy based on traditional acupuncture combined with modern electrotherapy in Asia. The present study aimed to determine the effects of EA treatment on spatial learning and memory impairment, and to elucidate the status of NOX2-related oxidative stress in a rat model of Alzheimer's disease induced by Beta-amyloid$_{1-42}$($A\beta_{1-42}$). Fifty-six adult female Sprague-Dawley (SD) rats were randomly divided into four groups: sham, sham+EA, AD and AD+EA. The rats in Sham+EA and AD+EA groups were respectively administrated EA treatment at Baihui and yongquan acupoints, once a day for 30 min, lasting for 28 days. The spatial learning and memory functions were assessed by Morris water maze (MWM) test. The activities of total antioxidant capacity (T-AOC), reactive oxygen species (ROS), malondialdehyde (MDA) and 8-hydroxy-2-deoxyguanosine (8-OH-dG) were evaluated. Moreover, the neuronal injury was detected by Nissl staining. Meanwhile, the NeuN expression was examined in the hippocampus, the expression levels of Nicotinamide adenine dinucleotide phosphate (NADPH)-oxidase2(NOX2) was detected by immunofluorescence staining and western blot. The results showed that EA treatment significantly improved spatial learning and memory impairment in rats induced by $A\beta_{1-42}$. Concomitantly, EA treatment markedly restored T-AOC and attenuated the abnormal increase in levels of ROS, MDA and 8-OH-dG in the hippocampus of the AD rats. More notably, EA treatment also effectively ameliorated neuronal injury and counteracted the aberrant increase of NOX2 levels in the hippocampus of AD rats. Our findings suggested that EA is a potential strategy for the treatment of AD, and the possible mechanism is associated with the alleviation of neuronal injury and inhibition of NOX2-related oxidative stress.

***Key words:*** Beta-amyloid$_{1-42}$($A\beta_{1-42}$); Spatial learning and memory impairment; Electroacupuncture(EA); Oxidative stress; NADPH oxidase 2( NOX2).

## Introduction

Alzheimer's disease (AD) is an age-dependent progressive and insidious neurodegenerative disorder marked by deficits in cognitive function. The neuropathology of AD is characterized by extracellular amyloid beta protein (Aβ) deposition, and neuro-fibrillary tangles-associated alteration of neuronal networks. Although several other hypotheses have been proffered to explain the changes in complex pathophysiological conditions of AD, such as amyloid cascade, excitotoxicity and inflammation, oxidative stress remains the most convincing explanation (1). The accumulated evidence indicates that extracellular Aβ peptide deposition causes an increase in intracellular reactive oxygen species (ROS)(2). The over generation of ROS results in structural and functional cell damage through lipid peroxidation and DNA damage (3). With so many of these harmful events in cells, oxidative stress involved in the pathogenesis of AD (4).

ROS can be generated in multiple intracellular compartments and regulated by multiple enzymes in cells. Nicotinamide adenine dinucleotide phosphate (NADPH) oxidase, an expanding family of ROS-generating enzymes including NOX1, NOX2, NOX3, NOX4, NOX5, DUOX1 and DUOX2, which share the capacity to transport electrons across the plasma membrane and to generate superoxide and other downstream ROS (5, 6). The activity of gp91phox, which is a catalytic subunit of NOX2, is strongly associated with ROS production (7). A recent study revealed that NOX2-derived ROS contributed to cognitive impairments induced by surgery in aged-mice (8). Another study found that inhibition of NOX2 could attenuate hydrogen peroxide-induced oxidative stress in HT22 cells (9).

Electroacupuncture (EA) treatment is a type of needling therapy, which combines traditional needling with electric stimulation. Clinically, EA treatment has been shown to have efficacy in curing many kinds of neurological diseases, such as depression (10, 11), cerebral ischemia-reperfusion injury (12) and stroke (13-15). It was reported that EA treatments accelerated the improvement of cognitive impairment in vascular dementia and ischemia-reperfusion injury in vivo experiments (16, 17). Repeated EA treatment could ameliorate spatial reference memory impairment in APP/PS1 double transgenic mice (12). While reviewing ancient Chinese documents regarding acupuncture and cognitive impairment, we discovered the GV20 and KI1 were the most frequently selected acupoints for treatment men-

tal disorders in China (16, 18, 19). Baihui (GV20; on the anterior midline in front of boundary of the frontal and parietal bones) and Yongquan (KI1; on center of the posterior palm) plays an important role in the nervous system. The GV20 acupoint is recognized to be involved in the improvement of headache, dizziness, fainting, and the K11 is involved in adjustment of memory function. Thus, using with an AD rat model induced by Beta-amyloid$_{1-42}$ (A$\beta_{1-42}$) intracerebroventrical injection, we expect to investigate whether EA treatment on GV20 and KI1 acupoints could improve spatial learning and memory impairment, and to explore the association of the potential therapeutic effects with inhibition of NOX2-related oxidative stress in AD rats.

## Materials and Methods

### Animals and groups

Fifty-six nulliparous female Sprague-Dawley rats (body weight: 290g-310g) were obtained from the Experimental Animal Centre of Sichuan University. The rats were housed in a temperature (~22°C) controlled room in which 12h light/dark cycle was maintained. The rats had free access to standard rodent chow and filtered water. After 7 days acclimation, the rats were randomly divided into 4 groups (n=14 each group): (1) sham group, rats were treated with bilaterally intracerebroventricular (ICV) injection of a water/acetonitrile (3:1) mixture; (2) sham+EA group, rats were treated with bilaterally ICV injection of a water/acetonitrile (3:1) mixture and EA treatment; (3) AD group, rats were treated with bilaterally ICV injection of Aβ1–42; (4) AD+EA group, rats were treated with bilaterally ICV injection of Aβ1-42 and EA treatment. The experiments were performed in accordance with the national guidelines for the care and use of laboratory animals and were approved by the Experimental Animal Welfare and Committee of Sichuan University.

### A$\beta_{1-42}$ oligomerization and AD rat model establishment

Beta-amyloid$_{1-42}$(A$\beta_{1-42}$ ), purchased from Abcam, Cambridge, MA, UK, was prepared at a concentration of 10mM in a 3:1 water/acetonitrile mixture, and aliquots were stored at –20°C. The A$\beta_{1-42}$ peptide oligomerization or a 3:1 water/acetonitrile mixture was administered by ICV injection, as previously described(20). Briefly, the rats were anesthetized with chloral hydrate (300mg/kg) via intraperitoneal injection and then placed on a stereotaxic apparatus (DW2000, Taimeng Co., Ltd., Chengdu, Sichuan, China). Burr holes were drilled in the skull on both sides over the lateral ventricles by using the following coordinates: 1.2mm posterior to the bregma, 2.0mm lateral to the sagittal suture, and 3.0mm beneath the surface of the dura. Total volume of 10μl of A$\beta_{1-42}$ (10mM) was intracerebroventriculy injected (5μl per lateral ventricle). Body temperature was maintained at 37°C by surface heating/cooling instrument (YGS230-II, Shanghai Tianshen Ltd., Shanghai, China).The injection lasted 30min and the needle with the syringe was left in place for 10min after the injection for the completion of drug infusion. After surgery, the scalp was sutured. Penicillin (100,000U) was injected intramuscularly into the gluteus, once a day for 3 days.

### EA treatment

EA treatment was performed immediately after A$\beta_{1-42}$ ICV injection, according to the method of reference (21). Briefly, the rats from the sham+EA and AD+EA groups were anesthetized with ethylether to avoid restraint stress. The rats were then stimulated with EA (G6805-II EA Instrument, Qingdao Xinsheng Co., Ltd., Qingdao, Shandong, China) at the Baihui acupoint (GV20) and Yongquan acupoints (KI1). The acupoint GV20 is located at the intersection of the sagittal midline and the line linking rat ears, and the acupoints KI1 are located at the center of the palm in posterior limbs. Acupuncture needles (0.18×30mm) were respectively inserted into GV20 and KI1 to a depth of approximately 5mm, then these needles were stimulated at an intensity of 1mA and at a frequency of 2/15Hz, once a day for 30min, lasting for 28 days. During the anesthesia and EA treatment period, the core temperature of rats was maintained at 37.0°C by surface heating or cooling instrument (YGS230-II, Shanghai Tianshen Co., Ltd., Shanghai, China). The rats in the sham and AD groups received anesthesia same as in the sham+EA and AD+EA groups, once a day for 28 days.

### Morris water maze test

To investigate spatial learning and memory ability, rats were subjected to the Morris water maze (MWM) test, including orientation navigation and space probe trials following 4 weeks of treatment (16, 22). Briefly, the MWM test was performed in a plastic, circular pool, 1.2m in diameter and 0.5m in height (WMT-100S, Taimeng Co., Ltd., Chengdu, Sichuan, China), which was filled with water (25±2°C) to a depth of 20cm. A circular platform (10cm in diameter) was placed in the fourth quadrant away from the edge of the pool. The top of the platform was submerged 1.5cm below the water surface. Water was made cloudy by adding milk powder. A video camera attached to a computer was placed above the center of the tank to record and analyze the trajectory of the rats (WMT-100S, Taimeng Co., Ltd., Chengdu, Sichuan, China). During the orientation navigation trials, each rat was gently placed in the water at one of the four equidistant locations in a random order. Then, the rat was allowed to swim escaping onto the platform, and the escape latency (the spending time to find the platform) was recorded for 60sec. After 60sec, if the rat failed to find the platform, it was guided to the platform and was allowed to stay on the platform for 20sec.The computer recorded the time it took the rat to find the platform. The orientation navigation trials were performed three trials a day with one starting at 8:00, the other at 14:00 and another at 20:00, and repeated for four days.

On the fifth day, the space probe test was conducted to assess memory consolidation, in which the platform was removed, and the rat was allowed to swim freely for 60sec. The start position was located 180˚ from the original platform position to ensure that the spatial preference was a reflection of the memory of the goal location, rather than for a specific swim path. The swimming time the rats spent in target quadrant were recorded. The percentage of time spent in the target quadrant was used for statistical analysis. After completion of the MWM test, rats in each group were sacrificed to harvest the

hippocampus for pathologic and biochemical analysis.

**ROS Staining**

ROS levels in the hippocampus were assessed using a ROS Fluorescent Probe-DHE kit (Beyotime, Jiangsu, China) according to the manufacturer's instructions(23). Briefly, the frozen hippocampus were cut at a thickness of 12μm, and then the sections were incubated with DHE (50μM) in PBS for 10min at 37°C in a humidified chamber protected from light. Fluorescent images were captured with a fluorescence microscope (Olympus, Tokyo, Japan). The ROS positive cells in hippocampus of each section were visualized following reaction with DHE, then using DAPI to visualize nuclei of all cells. The image selected for calculation of DHE-positive cells is 313×233μm$^2$ obtained by microscopy(LEICA, DFC310 FX) with a high-power lens(400×magnification).

**Immunofluorescence staining**

Rats were deeply anesthetized with 10% chloral hydrate (3ml/kg body weight, i.p.) and then fixed by transcardial perfusion with 0.9% NaCl, followed by 4% paraformaldehyde(Sigma, USA) and then the hippocampus were cut in 12μm sections. Subsequently, the sections were immersed in 0.3% $H_2O_2$ in methanol for 15min and then incubated with 10% normal goat serum for 30min. Afterwards, sections were incubated with primary antibodies: rabbit anti-neuron (1:200; Abcam, Cambridge, MA, UK), mouse anti-NOX2/gp91phox (1:200; Santa Cruz, USA) and mouse anti-8-hydroxy-2'-deoxyguanosine (8-OH-dG; 1:200; Santa Cruz, CA, USA) in 1% BSA at 4°C overnight in a humidified chamber. Following three washes with PBS, sections were then incubated with goat anti-rabbit IgG-FITC (1:600; proteintech, Chicago, IL, USA), donkey anti-mouse IgG-Cy3 (1:800; Abcam, Cambridge, MA, UK) and goat anti-mouse IgG-Cy3 (1:600; proteintech, Chicago, IL, USA) for 1h at room temperature. After washing out the secondary antibodies, sections were incubated with 4, 6-diamidino-2-pheny-lindole (DAPI; sigma, MO, USA) for nuclear staining. Fluorescent images were captured with a fluorescence microscope (Olympus, Tokyo, Japan). 8-OH-dG-positive cells were counted sham as the method mentioned in the section of ROS Staining.

**MDA content and total antioxidant capacity assay**

Lipid peroxidation was evaluated by malondialdehyde (MDA) assay kit (Jiancheng institute of biological engineering, Nanjing, Jiangsu, China) according to the manufacturer's instructions. Briefly, the hippocampus tissue was homogenized independently and centrifuged at 3500rpm for 10min. The supernatant was collected and incubated with MDA reaction solution and then measured by spectrophotometry at 532nm(24).

Total antioxidant capacity (T-AOC) was evaluated by T-AOC assay kit (Jiancheng institute of biological engineering, Nanjing, Jiangsu, China) according to the manufacturer's instructions. Briefly, the hippocampus tissue was homogenized independently and fully blending and keeping still for 10min.The supernatant was collected and was measured by spectrophotometry at 520nm.

**Nissl staining**

Rats were deeply anesthetized with 10% chloral hydrate and then fixed by transcardial perfusion with 0.9% NaCl, followed by 4% paraformaldehyde(Sigma, USA). After perfusion, the brain tissues were removed and post-fixed in the same solution at 4°Cfor overnight. Then, the specimens were processed and embedded in paraffin. Transverse serial sections were made and the blocks were cut at intervals of 30μm with 5μm in thickness of each section. For each level, one section was obtained and soaked in 1% toluidine blue (Beyotime, Nanjing, Jiangsu, China) for 3min. Sections were then dehydrated using 95% and 100% ethanol solutions, transparented using xylene, and placed the cover slips. Images were captured using a Mshot color video camera (MD50, China) mounted on an Olympus microscope (CX41, Japan).

**Western blot analysis**

The total protein of hippocampus was extracted as previously described(23). Briefly, the hippocampus tissue was homogenized independently in RIPA buffer (Beyotime, Nanjing, Jiangsu, China) with 1% Phenylmethylsulfonyl fluoride (PMSF) and protease inhibitor at 4°C. After centrifugation at 12,000rpm for 10min, the supernatant was collected and quantified by BCA (bicinchoninic acid) Protein Assay Kit (Beyotime, Nanjing, Jiangsu, China) and stored at -80°C. An equal amount of total protein (25mg) was loaded and separated by sodium dodecyl sulfate polyacrylamide gel and then transferred onto polyvinylidenefluoride (PVDF) membranes (Millipore, Billerica, MA, USA). The membranes were blocked with 5% non-fat milk in TBS-T(10 mmol/L Tris, 150 mmol/L NaCl and 0.1% Tween 20, pH 7.5) for 2h at room temperature, and the membranes were then incubated at overnight with different primary antibodies: mouse NOX2 antibody (1:200; Santa Cruze, USA), rabbit NeuN antibody (1:500; proteintech, Chicago,IL, USA), rabbit β-actin antibody (1:500; proteintech, Chicago,IL, USA). On the following day, the membranes were washed in TBS-T and incubated with the appropriate secondary antibodies conjugated to horseradish peroxidase (HRP) for 1h at room temperature. The target protein bands were visualized with chemiluminescence luminol reagents (ECL; millipore, Billerica, MA, USA). Blots were imaged by Molecular Image®ChemiDoc™ XRS+with Image Lab™ Software (Bio-Rad, Hercules, CA, USA). Quantitative data were obtained by ImageJ 1.50b Gel Analyzer (National Institutes of Health, Washington, DC, USA). Western blot data were normalized relative to the density of the β-actin bands.

**Statistical analysis**

All data were expressed as the mean±SD. A multifactorial analysis of variance (ANOVA) for repeated measurement was employed for analyzing escape latencies in the MWM test. One-way ANOVA was employed for analyzing other data followed by LSD (equal variances assumed) or Dunnett's T3 (equal variances not assumed) post hoc test with SPSS 17.0 software package. Statistical significance was set at $P<0.05$.

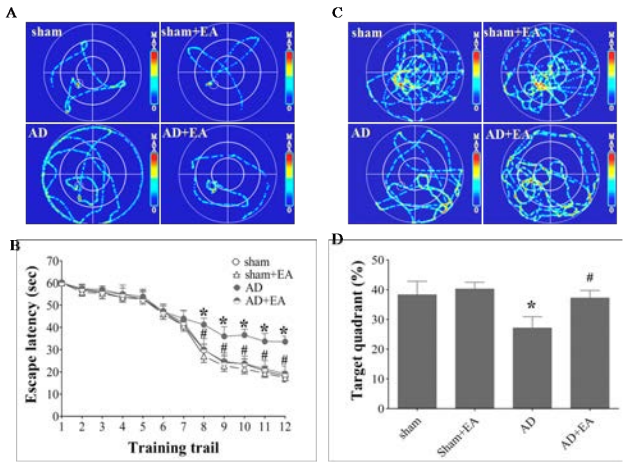


**Figure 1. EA treatment ameliorates $A\beta_{1-42}$-induced spatial learning and memory impairment in rats.** (A) photographs showed typical swimming patterns of rats in the sham, sham+EA, AD and AD+EA groups during orientation navigation trials. (B) The escape latency time of rats to find the platform during the training trials. (C) Typical swimming patterns of rats in the sham, sham+EA, AD and AD+EA groups during space probe trials. (D) Percentage of swimming time in the target quadrant where the platform has been located. The data arepresented as means ±SD (n=10). * $P$<0.05 vs. sham group; # $P$<0.05 vs. AD group.

## Results

### EA treatment ameliorates spatial learning and memory impairment induced by $A\beta_{1-42}$ in rats

To determine whether EA treatment could ameliorate spatial learning and memory impairment in AD rats, MWM test was applied and the results were shown in Figure 1. During the training period, the escape latency of all the tested rats was getting shorter and shorter as the learning proceeding. However, the escape latency of the rats in the AD group was consistently longer compared with those in the sham group (AD: 33.59±2.455s vs. sham: 18.14±2.064s, $P$<0.05), whereas EA treatment obviously decreased the escape latency of the AD rats (AD+EA: 19.09±3.493s vs. AD: 33.59±2.455s, $P$<0.05). In addition, there was not significantly different in escape latency between the sham and sham+EA groups (sham: 18.14±2.064svs. sham+EA: 17.33±1.866s, $P$>0.05; Figure 1A and 1B). In the space probe test, after removed the platform, the AD rats spent less time swimming in the target quadrant compared with those in the sham group (AD: 27.10±3.795% vs. sham: 38.28±4.496%, $P$<0.05). However, the rats in the AD+EA group spend more time swimming in the target quadrant than those in the AD group (AD+EA: 37.19±2.539% vs. AD: 27.10±3.795%, $P$<0.05). No significant difference was observed in the percentage of swimming time spent in the target quadrant between the sham and sham+EA groups(sham: 38.28±4.496%; sham+EA vs. 40.22±2.250%,$P$>0.05; Figure 1C and 1D). Thus, EA treatment could ameliorate the spatial learning and memory impairment induced by $A\beta_{1-42}$ in rats.

### EA treatment attenuates oxidative stress induced by $A\beta_{1-42}$ in rats

To explore whether EA treatment could attenuate oxidative stress in AD rats, the ROS was evaluated by using ROS Fluorescent Probe-DHE (Figure 2A). As illustrated in Figure 2B, the number of DHE-positive cells were strikingly increased in the AD group compared with the sham group (AD: 45.83±2.137 vs. sham: 13.50±1.871, $P$<0.05), whereas the increased DHE-positive cells due to $A\beta_{1-42}$ injection was decreased in the AD+EA group compared with the AD group (AD+EA:15.83±3.061 vs. AD:45.83±2.137, $P$<0.05). In addition, the number of DHE-positive cells in sham group did not differ significantly from the sham+EA groups (sham: 13.50±1.871 vs. sham+EA: 13.17±2.137, $P$>0.05).

Immunofluorescence staining revealed low levels and sparsely distributed 8-OH-dG immunoreactivity in the hippocampus of the sham rats (Figure 3A). In contrast, the 8-OH-dG immunoreactivity in the hippocampus in AD rats was strikingly increased. There was no identifiable difference in 8-OH-dG immunoreactivity in the hippocampus between the sham and AD+EA rats. As illustrated in Figrue 3B,the number of 8-OH-dG-positive cells was significantly increased in the AD group compared with sham group (AD: 8.00±2.191 vs. sham: 2.00±0.632, $P$<0.05). However, the number of 8-OH-dG-positive cells in the AD+EA group was significantly

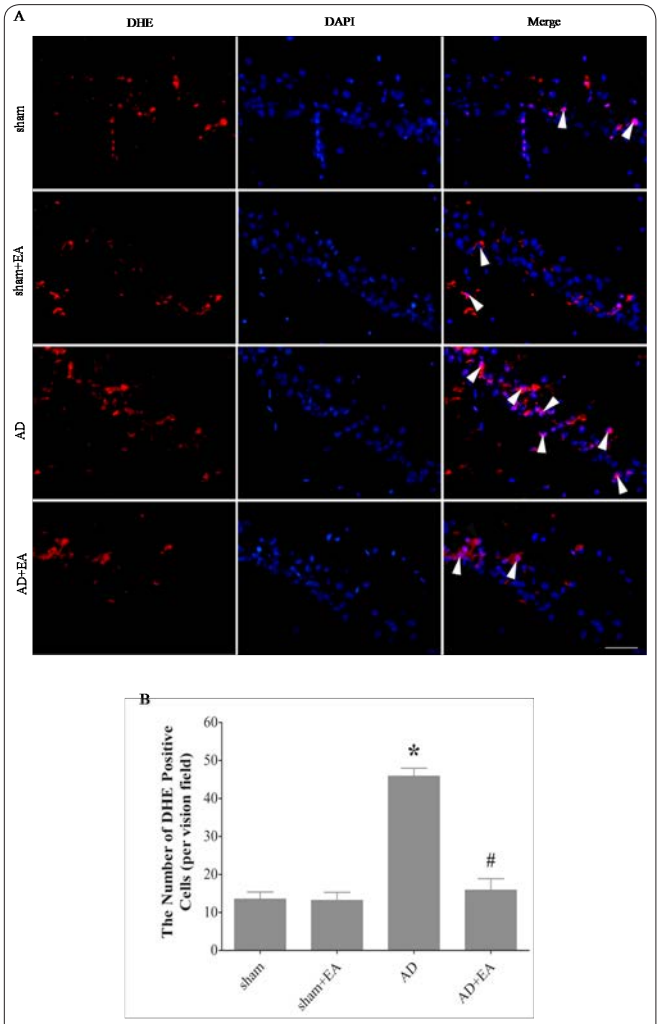


**Figure 2. EA treatment reduces ROS production induced by $A\beta_{1-42}$ injection in rats.** (A) Fluorescence images of DHE (red) and DAPI (blue) staining in rat hippocampus of the sham, sham+EA, AD and AD+EA groups. White arrow heads indicated the DHE-positive cells in the hippocampus. Scale bar=40μm. (B) Quantification of DHE-positive cells in the sham, sham+EA, AD and AD+EA groups. *$P$<0.05 vs. sham group; #$P$<0.05 vs. AD group. n=6, per group.

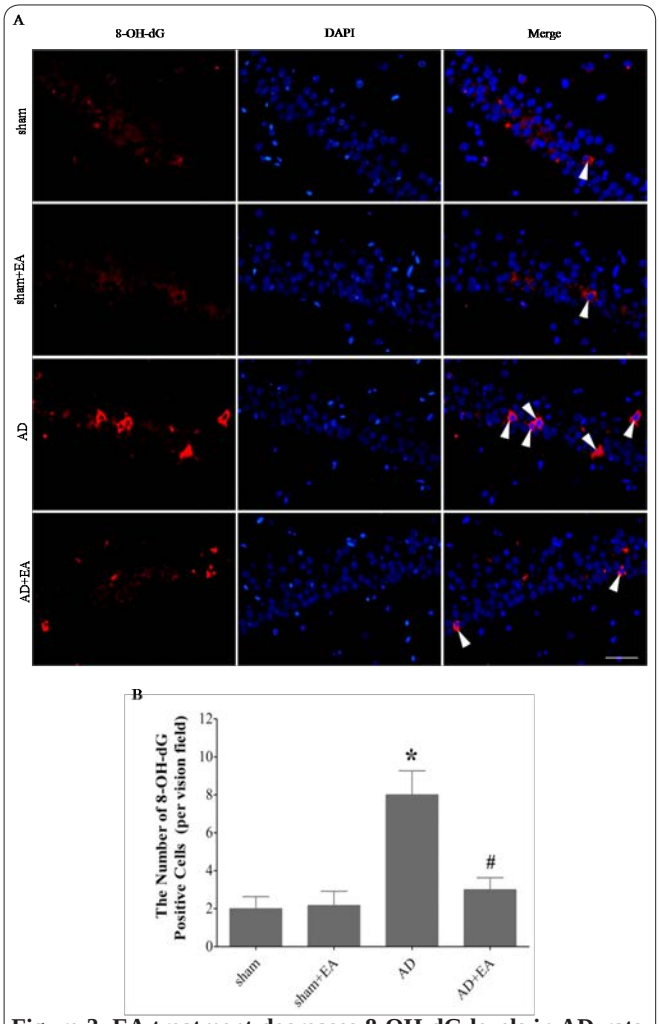


**Figure 3. EA treatment decreases 8-OH-dG levels in AD rats.** (A) Immunofluorescence staining for 8-OH-dG (red) and DAPI (blue) in the hippocampus of the sham, sham+EA, AD and AD+EA groups. White arrow heads indicated the 8-OH-dG-positive cells. Scale bar=40μm. (B) Quantification of the 8-OH-dG-positive cells in rat hippocampus of the sham, sham+EA, AD and AD+EA groups. **P*<0.05 vs. sham group; #*P*<0.05 vs. AD group. n=6, per group.

lower than that in the AD group (AD+EA: 3.00±0.632 vs. AD: 8.00±2.191, *P*<0.05). In addition, the difference in number of 8-OH-dG-positive cells had no statistical significance between the sham and sham+EA groups (sham: 2.00±0.632 vs. sham+EA : 2.17±0.753, *P*>0.05).

To further confirm the effects of EA treatment on lipid peroxidation induced by $A\beta_{1-42}$ injection, the MDA content was measured (Figure 4A). The MDA content was significantly increased in the AD group compared with the sham group (AD: 4.71±0.595nmol/mg prot vs. sham: 1.61±0.191nmol/mg prot, *P*<0.05). With EA treatment, however, the MDA content was significantly decreased in the EA+AD group compared with the AD group (EA+AD: 1.90±0.210nmol/mg prot vs. AD: 4.71±0.595nmol/mg prot, *P*<0.05). Moreover, the MDA contents did not vary significantly between the sham and sham+EA groups (sham: 1.61±0.191nmol/mg prot vs. sham+EA: 1.57±0.255nmol/mg prot, *P*>0.05).

In order to determine whether EA treatment could improve the anti-oxidative ability in AD rats, the T-AOC was assessed and the results were illustrated in Figure 4B. As compared to the sham group, the T-AOC was significantly decreased in the AD group (sham:

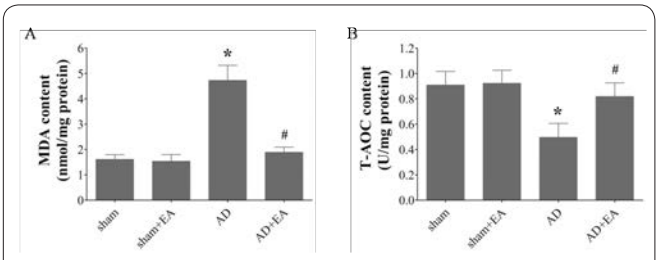


**Figure 4. Effect of EA treatment on MDA content and T-AOC in rat hippocampus.** (A) Comparisons of MDA content in rat hippocampus tissues of the sham, sham+EA, AD and AD+EA groups. (B) Comparisons of T-AOC in rat hippocampus tissues of the sham, sham+EA, AD and AD+EA groups. **P*<0.05 vs. sham group; # *P*<0.05 vs. AD group. n=8, per group.

0.91±0.115U/mg prot vs. AD: 0.50±0.118U/mg prot, *P*<0.05). In response to EA treatment, the T-AOC was strikingly increased (AD+EA: 0.82 ±0.116U/mg prot vs. AD:0.50±0.118U/mg prot, *P*<0.05). No significant difference was observed in T-AOC between the sham and sham+EA groups (sham:0.91±0.115U/mg prot vs. sham+EA:0.92±0.110U/mg prot, *P*>0.05). Taken together, EA treatment attenuates $A\beta_{1-42}$-induced oxidative stress in rats.

## EA treatment ameliorates neuronal injury and suppressesNOX2 expression in AD rats

To explore the possible mechanisms of EA treatment improved spatial learning and memory deficits in AD rat, the neuronal degeneration was detected by Nissl staining (Figure 5A). The neurons in the hippocampus of the sham and sham+EA groups exhibited normal shapes and deeply stained Nissl bodies. In the AD group, some of the neurons in the hippocampus became severely swollen and exhibited weakly stained Nissl bodies. With EA treatment, the swelling of neurons and Nissl bodies were obviously alleviated and stained more deeply in the AD+EA group.

The distribution of NOX2 was examined by double-label immunofluorescent staining of NOX2 and NeuN. As illustrated in Figure 5B, almost all the neurons expressed NOX2 in AD group when compared to the sham group. With EA treatment, the neurons with NOX2 and NeuN co-localization were markedly decreased in the AD+EA group. Quantitative analysis of the expression of NOX2 (Figure 5C) indicated that the level of NOX2 in the AD group was significantly increased compared with the sham group (AD: 1.14±0.052 vs. sham: 0.64±0.032, *P*<0.05). EA treatment significantly decreased the level of NOX2 in the AD+EA group compared to the AD group (AD+EA: 0.69±0.032 vs.AD: 1.14±0.052, *P*<0.05). Moreover, no significant difference in NOX2 expression was found between the sham and sham+EA groups (sham: 0.64±0.032 vs. sham+EA: 0.65 ±0.033, *P*<0.05). In contrast, the level of NeuN (Figure 5D) was significantly decreased in the AD group compared with that in the sham group (AD: 0.71±0.054 vs. sham: 0.99±0.051, *P*<0.05), whereas EA treatment strikingly increased the level of NeuN in the AD+EA group compared to the AD group (AD+EA: 0.94±0.071;AD: 0.71±0.054; *P*<0.05). These results demonstrated that EA treatment decreases NOX2 and increases NeuN expression in AD rats.

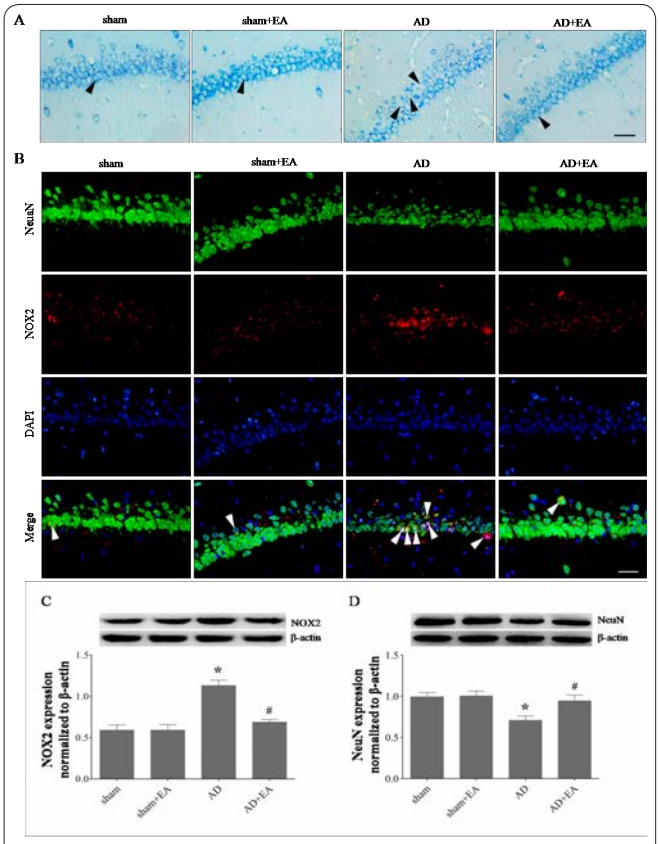


**Figure 5. EA treatment attenuates neuronal injury and suppresses NOX2 expression in AD rats.** (A)Nissl staining of the neurons in the hippocampus of the sham, sham+EA, AD and AD+EA groups. Scale bar=40μm. (B) Immunofluorescence images of NeuN and NOX2 staining in the hippocampus of the sham, sham+EA, AD and AD+EA groups. White arrow heads indicated NOX2-positive neurons in the hippocampus. Scale bar=40μm. (C) Quantification of NOX2 protein expression. (D) Quantification of NeuN protein expression.**P* < 0.05 vs. sham group, #*P* < 0.05 vs. AD group. n=6.

## Discussion

The results presented in this study suggested that GV20 and KI1EA stimulation could improve spatial learning and memory deficits induced by $A\beta_{1-42}$ in rats. Staining of DHE revealed that EA treatment effectively decreased ROS production in the hippocampus of AD rats, which was accompanied by a reduction of MDA and 8-OH-dG expression. Furthermore, the T-AOC was restored in the AD rats following EA treatment. More notably, EA treatment also attenuated neuronal injury, decreased the number of NOX2(+)/NeuN(+) cells and down-regulated NOX2 expression in AD rats. Our findings demonstrated that EA treatment could ameliorate spatial learning and memory impairment induced by$A\beta_{1-42}$ in rats, which might be associated with attenuation of neuronal degeneration in AD rats through inhibition of NOX2-related oxidative stress.

Experimental models of AD are essential to gaining a better understanding of pathogenesis and to perform preclinical testing of novel therapeutic approaches. Based on our research data and previous studies, it is recognized that the soluble Aβ oligomers rather than the final plaques may possess more severe neurotoxicity, since it is more likely to cause cognitive deficits in AD patients (25). Therefore, the rats subjected to intracerebroventricular injection of Aβ1-42 may be seen as an alternative to transgenic animals to study the AD mechanism, despite the fact that there is no presence of plaques in the brain of the model animals (26). Additionally, accumulating evidence showed that administration of soluble Aβ in mice/rats could induce cognitive deficits, inhibit LTP, and result in oxidative stress and neuronal loss hippocampus (27-29). Thus, we tended to choose this type of AD model in the current study.

Acupuncture therapy is a vital part of traditional medicine, and it has been shown to have significant clinical effects in the treatment of various diseases in Asia. A number of studies have demonstrated that the functions of the GV20 and KI1 acupoints in rats have similar physiological functions to those defined in patients. For example, some researches have conducted studying the effects of EA on GV20 and KI1 in treating cognitive impairment in rats, and several beneficial outcomes have been observed, including protection of neurological function by increased the expression of Bcl-2 and activation of the CREB signaling pathway (30), improved learning and memory performance via ameliorating the synaptic plasticity and efficiency of the excitatory synaptic transmission (31), decreased the activated glial cells (32), and attenuation of neuronal damage induced by hyper-gravity in rats (33), these results consistent with reports in the human (34, 35). . In the present study, with a widely used MWM test, we found that the spatial learning and memory abilities of rats in the EA+AD group were significantly improved compared to the AD group. Thus, this evidence suggested that EA treatment could effectively improve the learning and memory deficits induced by $A\beta_{1-42}$ in rats, which was consistent with previous research (12, 32).

ROS overproduction and oxidative stress have been proposed to play a critical role in AD (36). When ROS overwhelm the cellular antioxidant defense system, or a decrease in the cellular antioxidant capacity, oxidative stress occurs (37). Previous studies revealed that ROS is an instigator in Aβ production, which contributes to the characteristic neurodegeneration of AD (38, 39). We found that $A\beta_{1-42}$injection significantly increased the ROS level in the hippocampus of AD rats, and EA treatment had good alleviative effects. Several lines of evidence suggest that oxidative stress occurs in very early stages of AD ahead of massive Aβ deposits (26). The accumulated evidence indicate that oxidative stress not only damages essential cellular constituents such as lipids, proteins and nucleic acids, but also can decompose these products (40).The amounts of MDA often reflect the degree of lipid peroxidation in tissue and thus indirectly reflect the degree of cell damage (2). 8-OH-dG is one of the most sensitive DNA damage markers, and is produced following hydroxyl radical induction during oxidative stress (23). In this study, we found increase of MDA and 8-OH-dG expression in the hippocampus of AD rats, suggesting that oxidative stress occurs as a consequence of AD, there by potentially inducing spatial learning and memory deficit in AD rats. EA treatment notably decreased the accumulation of MDA and 8-OH-dG levels in the hippocampus of AD rats. T-AOC is an indicator of total intracellular antioxidant status, which indirectly reflect cell damage, and can be used to determine the degree of cell damage (41). In this study, we found that EA treatment strikingly increased the T-

AOC in the hippocampus of AD rats, suggesting that EA treatment attenuates oxidative stress induced by $A\beta_{1-42}$in rats. In this context, EA treatment has been shown to have antioxidant effects and to potentially improve spatial memory impairment.

The present study also demonstrated the neuoprotective effect of EA treatment based on the histopathological status of neurons in the hippocampus of AD rats. Nissl bodies are clumps of rough endoplasmic reticulum which are involved in the synthesis of proteins. Thus, staining of Nissl bodies is often used to reflect the functional status of neurons (42). We found that Nissl bodies of the neurons in the hippocampus of AD rats were deeply stained in sham rats. However, some of the neurons became swollen, and Nissl bodies were collapsed and stained lightly in the rats with $A\beta_{1-42}$ injection. After EA treatment, neuronal swelling became milder, and Nissl bodies were more deeply stained. These results suggest that EA treatment plays a significant role in alleviating neuronal injury induced by $A\beta_{1-42}$ in rats.

In order to investigate the mechanism of the neuroprotective action of EA, we examined the expression of NOX2. Nicotinamide adenine dinucleotide phosphate (NADPH) oxidases (NOXs) are a family of enzymes that lead to the generation of ROS (5) . It has been reported that gp91phoxis the catalytic subunit of NOX2.The activity of gp91phox is strongly associated with ROS production (23). Previous studies showed that EA treatment increased the activation of anti-oxidant enzymes (43), and attenuated brain injury through inhibition of NOX2 expression (23). In this study, the expression of gp91phox together with ROS production induced by $A\beta_{1-42}$ injectionis suppressed significantly by EA treatment. Our results were supported by a recent report that have been shown EA pretreatment inhibited NOX-mediated oxidative stress in mice with ischemic stroke (44). Thus, these results suggest that decreasing ROS generation with suppressing NOX2 expression is the possible mechanism of EA treatment to improve learning and memory impairment induced by $A\beta_{1-42}$ in rats.

In the present study, we only used Water maze test to assess learning and memory ability of rats. Previous research suggested that the Y-maze test is also a suitable method to evaluate the spatial learning and memory function of rats (26) . In addition, we only detected the neurons in the hippocampus, however, the presence and structure of glial cells and other associated proteins was not assessed. Therefore, the interpretation of the data is restricted by these limitations in the study design. However, the overall pattern in the data remains clear and the limitations will be addressed and improved in subsequent studies. Although more studies are still needed to fully elucidate the involvement of molecular signal pathways, our results strongly demonstrate that EA treatment can improve spatial learning and memory impairment via inhibition of NOX2-related oxidative stress and alleviation of neuronal injury in $A\beta_{1-42}$-induced AD rats. Our findings also suggest that EA at the GV20 and KI1 acupoints may serve as a promising strategy for AD treatment.

## Acknowledgements

This work was supported by National Natural Science Foundation of China (No. 11272225; 11572209).

## References

1. Martinez E, Navarro A, Ordonez C, Del Valle E, Tolivia J. Oxidative stress induces apolipoprotein D overexpression in hippocampus during aging and Alzheimer's disease. Journal of Alzheimer's disease : JAD2013;36:129-44.

2. Subash S, Essa MM, Al-Asmi A, Al-Adawi S, Vaishnav R, Braidy N, Manivasagam T, Guillemin GJ. Pomegranate from Oman Alleviates the Brain Oxidative Damage in Transgenic Mouse Model of Alzheimer's disease. Journal of traditional and complementary medicine2014;4:232-8.

3. Valko M, Leibfritz D, Moncol J, Cronin MT, Mazur M, Telser J. Free radicals and antioxidants in normal physiological functions and human disease. The international journal of biochemistry & cell biology2007;39:44-84.

4. Lyras L, Cairns NJ, Jenner A, Jenner P, Halliwell B. An assessment of oxidative damage to proteins, lipids, and DNA in brain from patients with Alzheimer's disease. Journal of neurochemistry1997;68:2061-9.

5. Bedard K, Krause KH. The NOX family of ROS-generating NADPH oxidases: physiology and pathophysiology. Physiological reviews2007;87:245-313.

6. Sorce S, Krause KH. NOX enzymes in the central nervous system: from signaling to disease. Antioxidants & redox signaling2009;11:2481-504.

7. Hernandes MS, D'Avila JC, Trevelin SC, Reis PA, Kinjo ER, Lopes LR, Castro-Faria-Neto HC, Cunha FQ, Britto LR, Bozza FA. The role of Nox2-derived ROS in the development of cognitive impairment after sepsis. Journal of neuroinflammation2014;11:36.

8. Qiu LL, Ji MH, Zhang H, Yang JJ, Sun XR, Tang H, Wang J, Liu WX, Yang JJ. NADPH oxidase 2-derived reactive oxygen species in the hippocampus might contribute to microglial activation in postoperative cognitive dysfunction in aged mice. Brain, behavior, and immunity2016;51:109-18.

9. Jia J, Ma L, Wu M, Zhang L, Zhang X, Zhai Q, Jiang T, Wang Q, Xiong L. Anandamide protects HT22 cells exposed to hydrogen peroxide by inhibiting CB1 receptor-mediated type 2 NADPH oxidase. Oxidative medicine and cellular longevity2014;2014:893516.

10. Zhang ZJ, Ng R, Man SC, Li JT, Wong W, Wong HK, Wang D, Wong MT, Tsang AW, Yip KC, Sze SC. Use of electroacupuncture to accelerate the antidepressant action of selective serotonin reuptake inhibitors: a single-blind, randomised, controlled study. Hong Kong medical journal = Xianggang yi xue za zhi2013;19 Suppl 9:12-6.

11. Weiner DK, Moore CG, Morone NE, Lee ES, Kent Kwoh C. Efficacy of periosteal stimulation for chronic pain associated with advanced knee osteoarthritis: a randomized, controlled clinical trial. Clinical therapeutics2013;35:1703-20 e5.

12. Wang F, Zhong H, Li X, Peng Y, Kinden R, Liang W, Li X, Shi M, Liu L, Wang Q, Xiong L. Electroacupuncture attenuates reference memory impairment associated with astrocytic NDRG2 suppression in APP/PS1 transgenic mice. Molecular neurobiology2014;50:305-13.

13. Yu KW, Lin CL, Hung CC, Chou EC, Hsieh YL, Li TM, Chou LW. Effects of electroacupuncture on recent stroke inpatients with incomplete bladder emptying: a preliminary study. Clinical interventions in aging2012;7:469-74.

14. Hsing WT, Imamura M, Weaver K, Fregni F, Azevedo Neto RS. Clinical effects of scalp electrical acupuncture in stroke: a sham-controlled randomized clinical trial. Journal of alternative and complementary medicine2012;18:341-6.

15. Sun J, Sang H, Yang C, Dong H, Lei C, Lu Y, Ma Y, Zhou X,

Sun X, Xiong L. Electroacupuncture improves orthostatic tolerance in healthy individuals via improving cardiac function and activating the sympathetic system. Europace : European pacing, arrhythmias, and cardiac electrophysiology : journal of the working groups on cardiac pacing, arrhythmias, and cardiac cellular electrophysiology of the European Society of Cardiology2013;15:127-34.
16. Lin R, Chen J, Li X, Mao J, Wu Y, Zhuo P, Zhang Y, Liu W, Huang J, Tao J, Chen LD. Electroacupuncture at the Baihui acupoint alleviates cognitive impairment and exerts neuroprotective effects by modulating the expression and processing of brain-derived neurotrophic factor in APP/PS1 transgenic mice. Molecular medicine reports2016;13:1611-7.
17. Li QQ, Shi GX, Yang JW, Li ZX, Zhang ZH, He T, Wang J, Liu LY, Liu CZ. Hippocampal cAMP/PKA/CREB is required for neuroprotective effect of acupuncture. Physiology & behavior2015;139:482-90.
18. Gemma M, Nicelli E, Gioia L, Moizo E, Beretta L, Calvi MR. Acupuncture accelerates recovery after general anesthesia: a prospective randomized controlled trial. Journal of integrative medicine2015;13:99-104.
19. Li F, Li LN, Wang X, Bai Y, Jiawula A, Bu QY, Gao TK, Xue WG. [Effect of electroacupuncture stimulation of "Baihui" (GV 20) and " Yongquan" (KI 1) on expression of hippocampal amyloid-beta and low density lipoprotein receptor-related protein-1 in APP/PS 1 transgenic mice]. Zhen ci yan jiu = Acupuncture research2015;40:30-4, 55.
20. Prakash A, Medhi B, Chopra K. Granulocyte colony stimulating factor (GCSF) improves memory and neurobehavior in an amyloid-beta induced experimental model of Alzheimer's disease. Pharmacology, biochemistry, and behavior2013;110:46-57.
21. Sun S, Chen X, Gao Y, Liu Z, Zhai Q, Xiong L, Cai M, Wang Q. Mn-SOD Upregulation by Electroacupuncture Attenuates Ischemic Oxidative Damage via CB1R-Mediated STAT3 Phosphorylation. Molecular neurobiology2016;53:331-43.
22. Tai DJ, Hsu WL, Liu YC, Ma YL, Lee EH. Novel role and mechanism of protein inhibitor of activated STAT1 in spatial learning. The EMBO journal2011;30:205-20.
23. Liu H, Zhao L, Yue L, Wang B, Li X, Guo H, Ma Y, Yao C, Gao L, Deng J, Li L, Feng D, Qu Y. Pterostilbene Attenuates Early Brain Injury Following Subarachnoid Hemorrhage via Inhibition of the NLRP3 Inflammasome and Nox2-Related Oxidative Stress. Molecular neurobiology2016.
24. Wang Y, Zhang C, Peng W, Xia Z, Gan P, Huang W, Shi Y, Fan R. Hydroxysaf fl or yellow A exerts antioxidant effects in a rat model of traumatic brain injury. Molecular medicine reports2016;14:3690-6.
25. Drummond E, Wisniewski T. Alzheimer's disease: experimental models and reality. Acta neuropathologica2017;133:155-75.
26. Ji XF, Chi TY, Xu Q, He XL, Zhou XY, Zhang R, Zou LB. Xanthoceraside ameliorates mitochondrial dysfunction contributing to the improvement of learning and memory impairment in mice with intracerebroventricular injection of abeta1-42. Evidence-based complementary and alternative medicine : eCAM2014;2014:969342.
27. Amin FU, Shah SA, Kim MO. Vanillic acid attenuates Abeta1-42-induced oxidative stress and cognitive impairment in mice. Scientific reports2017;7:40753.
28. Wang X, Wang L, Jiang R, Xu Y, Zhao X, Li Y. Exendin-4 antagonizes Abeta1-42-induced attenuation of spatial learning and memory ability. Experimental and therapeutic medicine2016;12:2885-92.
29. Zhao X, Liu C, Xu M, Li X, Bi K, Jia Y. Total Lignans of Schisandra chinensis Ameliorates Abeta1-42-Induced Neurodegeneration with Cognitive Impairment in Mice and Primary Mouse Neuronal Cells. PloS one2016;11:e0152772.
30. Han X, Zhao X, Lu M, Liu F, Guo F, Zhang J, Huang X. Electroacupuncture Ameliorates Learning and Memory via Activation of the CREB Signaling Pathway in the Hippocampus to Attenuate Apoptosis after Cerebral Hypoperfusion. Evidence-based complementary and alternative medicine : eCAM2013;2013:156489.
31. Jing XH, Chen SL, Shi H, Cai H, Jin ZG. Electroacupuncture restores learning and memory impairment induced by both diabetes mellitus and cerebral ischemia in rats. Neuroscience letters2008;443:193-8.
32. Zhu SX, Sun GJ. [Effects of electroacupuncture on learning and memory ability and glial cells of the hippocampus in the rat of Alzheimer disease]. Zhongguo zhen jiu = Chinese acupuncture & moxibustion2009;29:133-6.
33. Feng S, Wang Q, Wang H, Peng Y, Wang L, Lu Y, Shi T, Xiong L. Electroacupuncture pretreatment ameliorates hypergravity-induced impairment of learning and memory and apoptosis of hippocampal neurons in rats. Neuroscience letters2010;478:150-5.
34. Chou P, Chu H, Lin JG. Effects of electroacupuncture treatment on impaired cognition and quality of life in Taiwanese stroke patients. Journal of alternative and complementary medicine2009;15:1067-73.
35. Cheng HY, Cheng DQ. Progress in research on acupuncture treatment of senile dementia. Journal of traditional Chinese medicine = Chung i tsa chih ying wen pan2009;29:224-33.
36. Huang WJ, Zhang X, Chen WW. Role of oxidative stress in Alzheimer's disease. Biomedical reports2016;4:519-22.
37. Ray PD, Huang BW, Tsuji Y. Reactive oxygen species (ROS) homeostasis and redox regulation in cellular signaling. Cellular signalling2012;24:981-90.
38. Hardy J, Allsop D. Amyloid deposition as the central event in the aetiology of Alzheimer's disease. Trends in pharmacological sciences1991;12:383-8.
39. Zuo L, Hemmelgarn BT, Chuang CC, Best TM. The Role of Oxidative Stress-Induced Epigenetic Alterations in Amyloid-beta Production in Alzheimer's Disease. Oxidative medicine and cellular longevity2015;2015:604658.
40. Souza AC, Luchese C, Santos Neto JS, Nogueira CW. Antioxidant effect of a novel class of telluroacetilene compounds: studies in vitro and in vivo. Life sciences2009;84:351-7.
41. Wu FJ, Xue Y, Liu XF, Xue CH, Wang JF, Du L, Takahashi K, Wang YM. The protective effect of eicosapentaenoic acid-enriched phospholipids from sea cucumber Cucumaria frondosa on oxidative stress in PC12 cells and SAMP8 mice. Neurochemistry international2014;64:9-17.
42. Li XY, Xu L, Liu CL, Huang LS, Zhu XY. [Electroacupuncture Intervention Inhibits the Decline of Learning-memory Ability and Overex- pression of Cleaved Caspase-3 and Bax in Hippocampus Induced by Isoflurane in APPswe/PS 1]. Zhen ci yan jiu = Acupuncture research2016;41:24-30.
43. Siu FK, Lo SC, Leung MC. Electroacupuncture reduces the extent of lipid peroxidation by increasing superoxide dismutase and glutathione peroxidase activities in ischemic-reperfused rat brains. Neuroscience letters2004;354:158-62.
44. Jung YS, Lee SW, Park JH, Seo HB, Choi BT, Shin HK. Electroacupuncture preconditioning reduces ROS generation with NOX4 down-regulation and ameliorates blood-brain barrier disruption after ischemic stroke. Journal of biomedical science2016;23:32.